



# Aerobic capacity mediates susceptibility for the transition from steatosis to steatohepatitis

E. Matthew Morris<sup>1</sup> , Colin S. McCain<sup>1</sup>, Julie A. Allen<sup>1</sup>, Michelle L. Gastecki<sup>2</sup>, Lauren G. Koch<sup>3</sup>, Steven L. Britton<sup>3</sup>, Justin A. Fletcher<sup>4</sup>, Xiarong Fu<sup>4</sup>, Wen-Xing Ding<sup>5</sup>, Shawn C. Burgess<sup>4</sup>, R. Scott Rector<sup>2,6</sup> and John P. Thyfault<sup>1,7</sup> 

<sup>1</sup>Department of Molecular & Integrative Physiology, University of Kansas Medical Center, Kansas City, KS, USA

<sup>2</sup>Department of Nutrition and Exercise Physiology, University of Missouri, Columbia, MO, USA

<sup>3</sup>Department of Anesthesiology, University of Michigan, Ann Arbor, MI, USA

<sup>4</sup>Advanced Imaging Research Service, University of Texas Southwestern, Dallas, TX, USA

<sup>5</sup>Department of Pharmacology, Toxicology, and Therapeutics, University of Kansas Medical Center, Kansas City, KS, USA

<sup>6</sup>Harry S. Truman Memorial Veterans Hospital-Research Service, Columbia, MO, USA

<sup>7</sup>Kansas City VA Medical Center-Research Service, Kansas City, MO, USA

## Key points

- Low intrinsic aerobic capacity is associated with increased all-cause and liver-related mortality in humans.
- Low intrinsic aerobic capacity in the low capacity runner (LCR) rat increases susceptibility to acute and chronic high-fat/high-sucrose diet-induced steatosis, without observed increases in liver inflammation.
- Addition of excess cholesterol to a high-fat/high-sucrose diet produced greater steatosis in LCR and high capacity runner (HCR) rats. However, the LCR rat demonstrated greater susceptibility to increased liver inflammatory and apoptotic markers compared to the HCR rat.
- The progressive non-alcoholic fatty liver disease observed in the LCR rats following western diet feeding was associated with further declines in liver fatty acid oxidation and mitochondrial respiratory capacity compared to HCR rats.

**Abstract** Low aerobic capacity increases risk for non-alcoholic fatty liver disease and liver-related disease mortality, but mechanisms mediating these effects remain unknown. We recently reported that rats bred for low aerobic capacity (low capacity runner; LCR) displayed susceptibility to high fat diet-induced steatosis in association with reduced hepatic mitochondrial fatty acid oxidation (FAO) and respiratory capacity compared to high aerobic capacity (high capacity runner; HCR) rats. Here we tested the impact of aerobic capacity on susceptibility for progressive liver disease following a 16-week ‘western diet’ (WD) high in fat (45% kcal), cholesterol (1% w/w) and sucrose (15% kcal). Unlike previously with a diet high in fat and sucrose alone, the inclusion of cholesterol in the WD induced hepatomegaly and steatosis in both HCR and LCR rats, while producing greater cholesterol ester accumulation in LCR compared to HCR rats. Importantly, WD-fed low-fitness LCR rats displayed greater inflammatory cell infiltration, serum alanine transaminase, expression of hepatic inflammatory markers (F4/80, MCP-1, TLR4, TLR2 and IL-1 $\beta$ ) and effector caspase (caspase 3 and 7) activation compared to HCR rats. Further, LCR rats had greater WD-induced decreases in complete FAO and mitochondrial respiratory capacity. Intrinsic aerobic capacity had no impact on WD-induced hepatic steatosis; however, rats bred for low aerobic capacity developed greater hepatic inflammation, which was associated with reduced hepatic mitochondrial FAO and respiratory capacity and increased accumulation of cholesterol esters. These results confirm epidemiological reports that aerobic capacity impacts progression of liver disease and suggest that these effects are mediated through alterations in hepatic mitochondrial function.

(Received 6 March 2017; accepted after revision 4 May 2017; first published online 15 May 2017)

**Corresponding author** J. P. Thyfault: Department of Molecular and Integrative Physiology, 3901 Rainbow Boulevard, Hemenway Life Sciences Innovation Center, Mailstop 3043, University of Kansas Medical Center, Kansas City, KS 66160, USA. Email: jthyfault@kumcd.edu

**Abbreviations** ALT, alanine transaminase; ALP, alkaline phosphatase; AST, aspartate aminotransferase; CPT-1, carnitine palmitoyltransferase I; FAO, fatty acid oxidation; H&E, haematoxylin and eosin; HCR, high capacity runner; HFD, high fat diet; LCR, low capacity runner; LFD, low fat diet; MRC, mitochondrial respiratory capacity; MOMP, mitochondrial outer membrane permeability; NAFLD, non-alcoholic fatty liver disease; NASH, non-alcoholic steatohepatitis; TAG, triacylglycerol; WD, western diet.

## Introduction

Aerobic capacity, also termed cardiorespiratory fitness, is the most powerful predictor of cardiovascular and all-cause mortality independent of other major risk factors (Myers *et al.* 2002). Low aerobic capacity is also an independent predictor for multiple metabolic disease states including non-alcoholic fatty liver disease (NAFLD; Church *et al.* 2006). Aerobic capacity is substantially reduced in NAFLD patients (Crocì *et al.* 2012), and low initial aerobic capacity negatively impacts lifestyle-induced treatment of NAFLD (Kantartzis *et al.* 2009), increases mortality in chronic liver disease patients, and reduces survivability following liver transplant (Bernal *et al.* 2014). However, potential mechanisms by which aerobic capacity mediates susceptibility to NAFLD and liver disease are not well understood.

High calorie, high fat diets (HFD) are associated with NAFLD risk and obesity in humans and are commonly utilized to induce hepatic steatosis in rodent models. However, chronic HFD-induced hepatic steatosis does not progress to non-alcoholic steatohepatitis (NASH) in rodent models (Matteoni *et al.* 1999), whereas we and others have shown that the addition of refined sugar and/or cholesterol to an HFD induces NASH-like outcomes (Gan *et al.* 2014; Bashiri *et al.* 2016; Linden *et al.* 2016). Inappropriate cholesterol metabolism has received considerable attention in human and animal studies of NAFLD, and has been observed to modulate multiple pathways triggering NASH development (Min *et al.* 2012; Arguello *et al.* 2015). In support of these findings, large epidemiological reports link elevated cholesterol consumption with increased risk of NASH (Musso *et al.* 2003). Therefore, both intrinsic aerobic capacity and western diet (WD; high in fat, sugar and cholesterol) clearly impact prevalence and progression of NAFLD severity including the transition to NASH, but the interaction of these factors has never been examined.

In order to assess the role of intrinsic aerobic capacity in modulating the susceptibility to WD-induced NASH, we utilized the high capacity runner (HCR)/low capacity runner (LCR) rat model system created by selective breeding for divergent intrinsic aerobic capacities (Koch & Britton, 2001; Ren *et al.* 2013). We have previously shown

that low intrinsic aerobic capacity increases susceptibility for hepatic steatosis under chow and acute and chronic HFD conditions (increased lipids and sucrose), effects we have attributed to robust reductions in hepatic mitochondrial content, mitochondrial fatty acid oxidation (FAO) and mitochondrial respiratory capacity (MRC) in LCR vs. HCR rats (Thyfault *et al.* 2009; Morris *et al.* 2014, 2016). The robust differences in hepatic mitochondrial oxidative capacity play a role in the larger whole body differences in energy metabolism in the HCR/LCR rats that has been described by Britton, Koch and colleagues as the 'energy transfer hypothesis'. The hypothesis contends that high vs. low aerobic capacity leads to a greater rate of thermogenesis or metabolic entropy, and is supported by evidence that HCR rats have higher body and skeletal muscle temperature, higher resting energy expenditure, and greater mitochondrial metabolism in skeletal muscle and adipose. Here we tested the hypothesis that reduced intrinsic aerobic capacity and associated reductions in hepatic mitochondrial content, FAO and MRC would result in increased susceptibility for NASH in the LCR rats while the high-fitness HCR rats that display elevations in these hepatic mitochondrial features would be protected.

## Methods

### Animals

HCR/LCR rat development and characterization were previously described (Koch & Britton, 2001; Wisloff *et al.* 2005; Noland *et al.* 2007; Thyfault *et al.* 2009; Novak *et al.* 2010; Gavini *et al.* 2014; Morris *et al.* 2014; Vieira-Potter *et al.* 2015). Male rats (Generation 35) 25–30 weeks of age were singly housed ( $\sim 25^{\circ}\text{C}$ , 12-hour light cycle) with *ad lib* access to water, and acclimatized to the low-fat, control diet (LFD) (D12110704; 10% kcal fat, 3.5% kcal sucrose, 3.85 kcal  $\text{g}^{-1}$ ; Research Diets, Inc., New Brunswick, NJ, USA) for 2 weeks prior to the initiation of the western diet (WD) (D09071604; 45% kcal fat, 17% kcal sucrose, 1% cholesterol w/w, 4.68 kcal  $\text{g}^{-1}$ ; Research Diets, Inc.). Food intake and body weight were monitored weekly during a 16-week dietary intervention ( $n = 8$  in each group). Animals were anaesthetized with pentobarbital (75 mg  $\text{kg}^{-1}$ , i.p.) prior to killing by exsanguination

and bilateral thoracotomy. Tissues were collected and snap frozen in liquid nitrogen after an overnight fast. The animal protocols were approved by the Institutional Animal Care and Use Committee at the University of Missouri and the Subcommittee for Animal Safety at the Harry S. Truman Memorial VA Hospital.

### Body composition analysis

Body composition was measured by magnetic resonance using the EchoMRI-900 analyser (EchoMRI, Houston, TX, USA). Body composition was determined before the initiation of WD and periodically throughout the 16-week dietary intervention.

### Liver lipid analysis

Liver triacylglycerol concentration was determined as previously described using a commercially available kit (F6428, Sigma-Aldrich, St Louis, MO, USA) (Thyfault *et al.* 2009). Liver cholesterol was determined utilizing a commercially available kit (ab65359, Abcam, Cambridge, MA, USA).

### Liver histochemical staining

Haematoxylin and eosin (H&E) staining was performed as described previously (Rector *et al.* 2010).

### Mitochondrial isolation

Mitochondria were isolated from rat liver tissue, as previously described (Morris *et al.* 2012). Briefly, tissue was homogenized (Teflon on glass) in cold liver mitochondrial isolation buffer (220 mannitol, 70 sucrose, 10 mM Tris, and 1 mM EDTA, adjusted to pH 7.4 with KOH) and centrifuged (1500 *g*, 10 min, 4°C). The supernatant was serially centrifuged (8000 *g*–6000 *g*–4000 *g*, 10 min, 4°C), with the pellet resuspended (glass on glass) in liver mitochondrial isolation buffer following each centrifugation. The protein concentration was determined by bicinchoninic acid assay.

### Mitochondrial respiration

Mitochondrial oxygen consumption was measured using a Clark-type electrode system (Strathkelvin Instruments, North Lanarkshire, UK) as previously described (Morris *et al.* 2013). The consumption of oxygen in nmol min<sup>-1</sup> was normalized to mitochondrial protein in the respirometer cell.

### Palmitate oxidation by liver homogenate

The oxidation of [1-<sup>14</sup>C]palmitate was measured in fresh liver homogenates as previously described (Morris

*et al.* 2012). Fatty acid oxidation was assessed by measuring the production of <sup>14</sup>CO<sub>2</sub> (complete FAO) and <sup>14</sup>C-acid-soluble metabolites in a sealed trapping device at 37°C containing palmitate (200 μM). In order to approximate the carnitine palmitoyltransferase I (CPT-1)-mediated and non-CPT-1-mediated FAO in the liver homogenate, parallel incubations were included with the CPT-I inhibitor etomoxir (100 μM). One animal for each group was analysed daily. Values were normalized to the wet weight of the liver tissue sample.

### Pyruvate oxidation by isolated mitochondria

The oxidation of 5 mM pyruvate ([2-<sup>14</sup>C]pyruvate) to <sup>14</sup>CO<sub>2</sub> by isolated liver mitochondria was used to monitor pyruvate oxidation and approximate tricarboxylic acid (TCA) cycle flux as previously described (Morris *et al.* 2012).

### Acyl-carnitine analysis

Plasma and liver acyl-carnitines were measured by liquid chromatography–tandem mass spectrometry (LC-MS/MS) on an API 3200 triple quadrupole mass spectrometer (Applied Biosystems/Sciex Instruments, Foster City, CA, USA) as previously described (Satapati *et al.* 2012). Briefly, liver and plasma free carnitine and acyl-carnitines were extracted, derivatized, and individual acyl-carnitine peaks were then quantified by comparison with a <sup>13</sup>C internal standard (Cambridge Isotopes, Andover, MA, USA). Liver metabolites were normalized to tissue sample weight.

### Citrate synthase activity

Citrate was determined as previously described (Srere, 1969). Values were normalized to the wet weight of the liver tissue sample.

### Liver nucleotides

Liver ATP, ADP and AMP were measured by mass spectrometry as described previously (Satapati *et al.* 2015). Briefly, frozen liver samples were spiked with [<sup>13</sup>C<sub>10</sub>,<sup>15</sup>N<sub>5</sub>]ATP and [<sup>13</sup>C<sub>10</sub>,<sup>15</sup>N<sub>5</sub>]AMP (Sigma-Aldrich) internal standards before extraction. Analysis was performed on an API 3200 triple quadrupole mass spectrometer in positive electrospray ionization mode. A reverse-phase C18 column (Waters xBridge, 150 × 2.1 mm, 3 μm) and a gradient elution consisting of water/methanol (5:95, v/v) with 4 mM dibutylamine acetate (eluent A) and acetonitrile with 4 mM dibutylamine acetate (eluent B) was used to achieve separation. Nucleotides were quantified in standard solutions and samples by positive-ion-mode electrospray ionization and

**Table 1. SYBR RT-PCR primers used in the study**

Gene	Forward primer	Reverse primer
CycB ( <i>PPIB</i> )	CTTAGCTACAGGAGAGAAAGG	TTCAGCTTGAAGTTCTCCATC
F4/80 ( <i>EMR1</i> )	GGAGGACCAATGTCCAGGG	TGGGCAAGAACAGCTGTAGG
MCP-1 ( <i>CCL2</i> )	GAAGCTGTAGTATTTGCACC	TTCTAATGTACTTCTGGACCC
<i>IL1B</i>	TAAGCCAACAAGTGGTATTC	AGGTATAGATTCTTCCCCTTG
<i>TLR2</i>	AAAAACTGCTGAGATTTTGC	TACTAACATCCAACACCTCC
<i>TLR4</i>	ACCTAGATCTGAGCTTCAAC	TTGTCTCAATTTACACCTG
<i>TLR9</i>	AACCTCAGCCATAACATCC	ACTTCCAGCAGTAAGTCTAC
<i>CPT1a</i>	CCTACCACGGCTGGATGTTT	TACAACATGGGCTCCGACC
<i>HADHA</i>	ACAGGTTTACAAAACAGTGG	CTCTCAAATTTCTCTGATTCTG
<i>HMGCR</i>	GCCTCCATTGACATCCGGAGG	AGGGATGGGAGGCCACAAAG
<i>SOAT1</i>	CTCATATGTCAGAGAGAATGTG	AACTGCATAGCAACATAACC
<i>SOAT2</i>	GGTCAGATTCTGATGAAAAG	CCACATAATTCACCTGATG
<i>CES1d</i>	GAGATCCTGACTGAGAAGAG	CTCAGAGATTTTCAGTGTGG
<i>CES1e</i>	TTCTGCCAACAAATGATGAAC	GTTGGTCTTTATTTCTGTCTGG
<i>nCEH1</i>	TGGCCACTGCAAAAAATCAGC	AGGAAGTATTTGGTGGCCCA
<i>CYP7a1</i>	GCGAAGGCATTTGGACACAG	ACCCAGGCATTGCTCTTTGA
<i>CYP17a1</i>	GGCGACAGAAATCTGGTGGA	TGTCCATCAGGTGGAGATA
<i>HSD17b</i>	AAGAGCTTGCCAAATGGGGA	TCTCTCATGACCCGGGA
<i>SRD5a1</i>	GTGGTTAGTGGGCATGGTGA	ATTCAAACAGGCCTCCCCTG
<i>ABCG5</i>	CCCTTTGATTTCTACATGGAC	GTTCTTTCAATGTTCTCCAGG
<i>ABCG8</i>	AACAACCTGTGGATAGTACC	GATGGCATAAAGAGGATGTG
<i>ABCA1</i>	GGGAGAGAATGCTGAATATC	CATCTGAAAAACAGGTTTGG
SR-B1 ( <i>SCARB1</i> )	CATTCTTGTCTTAGACATC	GACGGATTTGATGTACAGAC
<i>LDLR</i>	CAGTGTGAAGATATTGACGAG	TCATCTTACGTACCTCATGG
BSEP ( <i>ABCB11</i> )	TGGGGCTCGTCAGATAAGGA	ACATGCGCTGGAGGAAATGA
NTCP ( <i>SCL10A1</i> )	CATTCAACTCTGTTCTACCATC	TTTTGTTTGGTCCCTTTG
<i>TGFb</i>	GGAAATCAATGGGATCAGTC	CTGAAGCAGTAGTTGGTATC
<i>COL1a</i>	TGGATTCCAGTTCGAGTATG	AGTGATAGGTGATGTTCTGG
<i>TNFa</i>	CTCACACTCAGATCATCTTC	GAGAACCTGGGAGTAGATAAG
<i>CD11c</i>	CAAAGCTGAGCTGGGAGACA	TGGCTGCTGATGACAGTGTA
<i>CD163</i>	TGTAGTTTCAATCTTCGGTCC	CACCTACCAAGCGGAGTTGAC
<i>CD68</i>	TCACAAAAAGGCTGCCACTCTT	TCGTAGGGCTTCGTTGCTGTGCTT
<i>CD64</i>	GGACAGTGCGAATACAGGT	CTTCTGTGAGGACTCTGCGG
DR5 ( <i>TNFRSF10B</i> )	CATTAGGAAGGAAGTTGCTG	CATTTGGTACAAGACCTCAC
<i>Fas</i>	ATTATAAGCTCCTTTGGCTG	CATCTGAGACATTCATTGGC
<i>TNFRSF1a</i>	CTCCATACATTTGTAGGGATTC	GGAGTTAGGGGCTTAGTAAC
<i>NLRP3</i>	AAGAGGAGTGGATAGGTTTA	CTGTCTTTGATGGAGTAGAAC

multiple reaction monitoring. Liver nucleotides were normalized to tissue sample weight. Liver energy charge was calculated as  $([ATP] + \frac{1}{2}[ADP])/([ATP] + [ADP] + [AMP])$ .

### Western blotting

Triton X-100 cell lysates were used to produce Western blot-ready Laemmli samples. Samples were separated by SDS-PAGE, transferred to polyvinylidene difluoride membrane and probed with primary antibodies. Bcl-2, Bcl-xL, Bax, Bak, caspase 3 and caspase 7 antibodies were purchased from Cell Signaling Technology (Danvers, MA, USA). HADHA antibody was purchased from Abcam. CPT-1a antibody was purchased from Proteintech Group,

Inc. (Rosemont, IL, USA). Individual protein bands were quantified using a densitometer (Bio-Rad Laboratories, Hercules, CA, USA) and protein loading was corrected by 0.1% amido-black (Sigma-Aldrich) staining to determine total protein as previously described (Morris *et al.* 2012).

### mRNA expression

RNA and cDNA were prepared as previously described (Morris *et al.* 2013). Real time quantitative PCR analysis was performed utilizing a Prism 7000 (ThermoFisher Scientific, Waltham, MA, USA) and SYBR green rat primers (Sigma Aldrich, St. Louis, MO, USA) (Table 1). All gene specific values were normalized to relative cyclophilin B mRNA expression values.

**Table 2. Animal characteristics following 16 weeks' of low-fat diet (LFD) or western diet (WD) for high capacity runner (HCR) and low capacity runner (LCR) rats**

	HCR		LCR	
	LFD	WD	LFD	WD
<b>Anthropometrics</b>				
Final body weight (g)	436.9 ± 23.6	460.5 ± 19.2	511.6 ± 29.5*	560.8 ± 32.8*
Weight gain (g)	50.8 ± 6.9	82.7 ± 9.7 <sup>†</sup>	34.1 ± 7.1	88.9 ± 14.2 <sup>†</sup>
Body fat %	19.3 ± 1.5	21.6 ± 1.5	24.6 ± 1.7*	26.8 ± 1.5*
Change in body fat %	5.5 ± 1.2	6.3 ± 0.8	6.9 ± 0.9	10.2 ± 0.4**, <sup>††</sup>
Energy intake (weekly average, kcal) <sup>a</sup>	387.8 ± 15.5	431.5 ± 10.6 <sup>††</sup>	394.7 ± 22.3	424.9 ± 18.9
Feed efficiency (weekly average, mg kcal <sup>-1</sup> ) <sup>b</sup>	9.3 ± 1.4	11.4 ± 1.4	6.4 ± 1.5	11.9 ± 1.4 <sup>††</sup>
Liver weight (g)	9.2 ± 0.5	18.2 ± 1.2 <sup>†</sup>	9.9 ± 0.6	17.6 ± 1.4 <sup>†</sup>
<b>Serum</b>				
ALT (U l <sup>-1</sup> )	45.4 ± 4.2	126.1 ± 25.6 <sup>†</sup>	51.6 ± 9.9	206.1 ± 30.6 <sup>†, **</sup>
AST (U l <sup>-1</sup> )	99.8 ± 10.2	196.6 ± 38.1 <sup>†</sup>	96.3 ± 11.5	238.9 ± 29.0 <sup>†</sup>
ALP (U l <sup>-1</sup> )	118.0 ± 6.4	133.4 ± 10.2	71.0 ± 4.5**	118.3 ± 6.1 <sup>††</sup>
Cholesterol (mg dl <sup>-1</sup> )	86.1 ± 6.4	92.1 ± 16.7	98.1 ± 7.9	134.0 ± 8.6**, <sup>††</sup>
<b>Plasma</b>				
Glucose (mg dl <sup>-1</sup> )	169.1 ± 8.5	174.5 ± 7.4	172.5 ± 9.9	167.9 ± 5.1
Insulin (ng ml <sup>-1</sup> )	1.39 ± 0.18	1.47 ± 0.19	1.08 ± 0.17	1.37 ± 0.21

Data are means ± SEM ( $n = 8$ ). <sup>a</sup>Average weekly energy intake during the 16 weeks' diet. <sup>b</sup>Weekly feed efficiency as weekly body weight gain divided by weekly energy intake. \* $P < 0.05$  main effect HCR vs. LCR; <sup>†</sup> $P < 0.05$  main effect LFD vs. WD; \*\* $P < 0.05$  HCR vs. LCR within diet; <sup>††</sup> $P < 0.05$  LFD vs. WD within strain. ALP, alkaline phosphatase; ALT, alanine transaminase; AST, aspartate aminotransferase.

## Statistical analysis

Animals within strain were randomized by weight into the two dietary groups. The main effects of phenotype and diet were tested by using 2-way ANOVA (SPSS Statistics, IBM, Armonk, NY, USA). Where significant main effects were observed, *post hoc* analysis was performed using least significant difference to test for any specific pairwise differences. Statistical significance was set at  $P < 0.05$ .

## Results

### Animal characteristics

Final body weight was ~16% less in HCR compared to LCR rats regardless of diet (Table 2,  $P < 0.05$ ). However, 16 weeks of WD produced significant weight gain in both HCR and LCR rats compared to LFD (~60% in each strain,  $P < 0.05$ ). The LCR rats displayed ~20% higher body fat percent than HCR rats across all diets ( $P < 0.05$ ). Interestingly, WD caused no change in body fat percent in the HCR rats, but caused a ~50% increase in the LCR rats ( $P < 0.05$ ). WD significantly increased liver weight in both HCR and LCR rats compared to LFD (~2 fold in each strain,  $P < 0.05$ ).

### Fasting serum and plasma

Circulating glucose and insulin (Table 2) were not different among groups. WD resulted in a significant > 2-fold

increase in aspartate aminotransferase (AST) in both strains and a 2-fold and 4-fold increase in alanine transaminase (ALT) in HCR and LCR rats, respectively ( $P < 0.05$ ), representing a ~60% greater ALT in LCR compared to HCR rats ( $P < 0.05$ ). Alkaline phosphatase (ALP) levels were ~40% lower in LCR compared to HCR rats on LFD ( $P < 0.05$ ), and only LCR rats displayed an increase following WD (67%,  $P < 0.05$ ). Finally, the WD diet increased serum cholesterol levels only in the LCR rats (37%,  $P < 0.05$ ). In summary, reduced intrinsic aerobic capacity results in WD-induced increases in body fat and serum markers of liver damage.

### Liver histology and lipid analysis

Liver H&E images show increased steatosis in both strains following chronic WD (Fig. 1A); however, the LCR rats displayed greater increases in inflammatory cell infiltration than the HCR rats following WD feeding. While differences in fibrosis markers, namely transforming growth factor  $\beta$  (*TGF $\beta$* ) and collagen, type I,  $\alpha$  1 (*Col1a1*) mRNA expression, were observed due to the WD in both strains (data not shown), no difference was observed in picrosirius red staining for fibrosis due to either strain or diet. Unlike previous observations (Thyfaut *et al.* 2009; Morris *et al.* 2014, 2016), liver triacylglycerol (TAG) content was found to be higher in HCR compared to LCR rats on LFD (Fig. 1B, ~35%,  $P < 0.05$ ). Chronic WD resulted in a > 3.5-fold increase

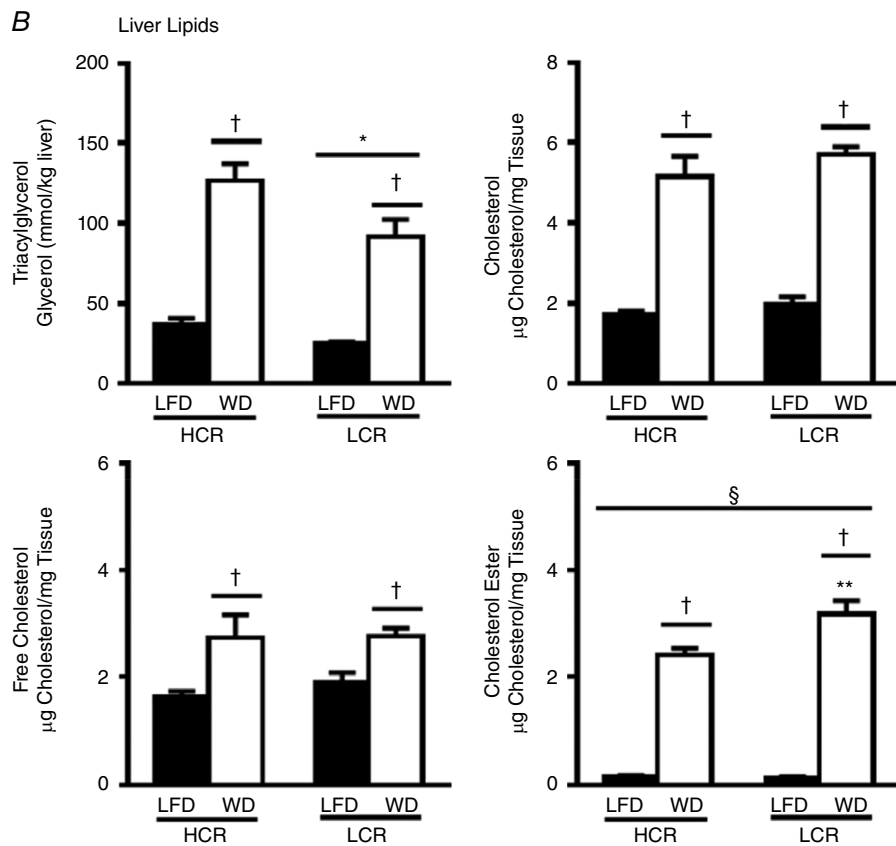
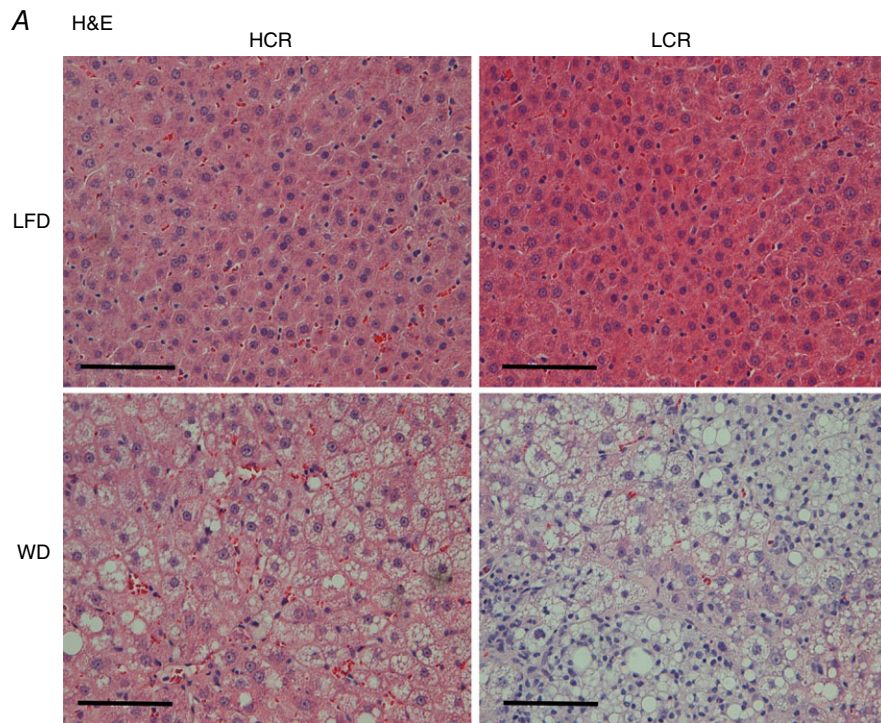


**Figure 1. High intrinsic aerobic capacity protects against high-fat/high-cholesterol diet-induced hepatic steatosis and non-parenchymal cellular infiltration**

*A*, representative H&E images. Scale bars represent 50  $\mu\text{m}$ . *B*, liver triacylglycerol, total cholesterol, free cholesterol and cholesterol ester determined biochemically. Values are means  $\pm$  SEM ( $n = 8$ ).  $\S P < 0.05$  interaction;  $*P < 0.05$  main effect HCR vs. LCR;  $\dagger P < 0.05$  main effect LFD vs. WD,  $**P < 0.05$  HCR vs. LCR within diet.

**Table 3. mRNA expression of genes for liver cholesterol metabolism, bile acid metabolism, transporters and inflammation**

Gene	HCR		LCR		Interaction
	LFD	WD	LFD	WD	
<b>Cholesterol ester metabolism</b>					
<i>HMGCR</i>	1.01 ± 0.06	0.60 ± 0.06 <sup>††</sup>	0.47 ± 0.04*	0.43 ± 0.05*	<i>P</i> < 0.002
<i>SOAT1</i>	1.03 ± 0.11	3.25 ± 0.71 <sup>†</sup>	0.94 ± 0.08	2.69 ± 0.45 <sup>†</sup>	NS
<i>SOAT2</i>	1.01 ± 0.04	0.62 ± 0.04 <sup>††</sup>	0.87 ± 0.07*	0.89 ± 0.03*	<i>P</i> < 0.001
<i>nCEH1</i>	1.01 ± 0.06	1.19 ± 0.11	1.82 ± 0.21*	1.80 ± 0.18*	NS
<i>CES1d</i>	1.07 ± 0.14	1.33 ± 0.29	0.93 ± 0.10	1.04 ± 0.17	NS
<i>CES1e</i>	1.00 ± 0.04	0.96 ± 0.11	1.23 ± 0.08*	1.12 ± 0.12*	NS
<b>Bile acid/steroidogenesis</b>					
<i>CYP7a1</i>	1.10 ± 0.17	1.44 ± 0.15	0.44 ± 0.07*	3.80 ± 0.64 <sup>*,††</sup>	<i>P</i> < 0.0001
<i>CYP17a1</i>	1.08 ± 0.26	0.41 ± 0.08 <sup>††</sup>	0.98 ± 0.21	0.85 ± 0.25	NS
<i>HSD17b</i>	0.93 ± 0.13	0.58 ± 0.09 <sup>††</sup>	1.51 ± 0.26*	2.65 ± 0.47 <sup>*,††</sup>	<i>P</i> < 0.02
<i>SRD5a1</i>	1.05 ± 0.13	0.30 ± 0.03	0.83 ± 0.8	0.31 ± 0.11	NS
<b>Cholesterol/bile transporters</b>					
<i>ABCG5</i>	1.08 ± 0.16	1.86 ± 0.35 <sup>††</sup>	0.74 ± 0.14	0.92 ± 0.17 <sup>**</sup>	NS
<i>ABCG8</i>	1.07 ± 0.16	0.60 ± 0.17 <sup>†</sup>	2.65 ± 0.53*	1.26 ± 0.23 <sup>*,†</sup>	NS
<i>ABCA1</i>	1.02 ± 0.08	1.18 ± 0.06	1.00 ± 0.11	1.64 ± 0.15 <sup>*,††</sup>	<i>P</i> < 0.05
<i>SR-B1 (SCARB1)</i>	1.03 ± 0.09	0.80 ± 0.05 <sup>††</sup>	1.06 ± 0.07	1.04 ± 0.08 <sup>**</sup>	NS
<i>LDLR</i>	1.03 ± 0.09	0.35 ± 0.06 <sup>†</sup>	0.91 ± 0.06	0.41 ± 0.02 <sup>†</sup>	NS
<i>BSEP (ABCB11)</i>	1.01 ± 0.05	0.88 ± 0.07 <sup>†</sup>	1.33 ± 0.05*	1.03 ± 0.10 <sup>*,†</sup>	NS
<i>NTCP (SCL10A1)</i>	1.01 ± 0.05	0.52 ± 0.06 <sup>†</sup>	1.03 ± 0.10	0.70 ± 0.07 <sup>†</sup>	NS
<b>Inflammation</b>					
<i>NLRP3</i>	1.09 ± 0.18	2.38 ± 0.41 <sup>†</sup>	0.87 ± 0.08	2.81 ± 0.33 <sup>†</sup>	NS
<i>TNFA</i>	0.94 ± 0.11	3.39 ± 0.60 <sup>†</sup>	0.69 ± 0.08	5.26 ± 1.33 <sup>†</sup>	NS
<i>CD11c</i>	1.00 ± 0.06	3.27 ± 0.46 <sup>†</sup>	0.78 ± 0.12	4.04 ± 0.67 <sup>†</sup>	NS
<i>CD68</i>	1.08 ± 0.15	2.38 ± 0.40 <sup>†</sup>	0.81 ± 0.06	2.56 ± 0.36 <sup>†</sup>	NS
<i>CD64</i>	0.94 ± 0.11	1.59 ± 0.20 <sup>†</sup>	0.83 ± 0.07	1.89 ± 0.25 <sup>†</sup>	NS

Gene expression in liver was determined by RT-PCR. Relative expression of listed genes related to liver bile acid metabolism and inflammation state were normalized to cyclophilin B (*PP1B*) and presented as means ± SEM (*n* = 7–8). \**P* < 0.05 main effect HCR vs. LCR; †*P* < 0.05 main effect LFD vs. WD; \*\**P* < 0.05 HCR vs. LCR within diet; ††*P* < 0.05 LFD vs. WD within strain.

in liver TAG and increases in liver weight in both strains (*P* < 0.05). The HCR rats maintained 38% greater liver TAGs compared to LCR rats after the WD diet (*P* < 0.05). Total liver cholesterol was increased ~3-fold in both strains following WD (Fig. 1B, *P* < 0.05), and hepatic free cholesterol was increased 67% in HCR and 45% in LCR rats (*P* < 0.05). Hepatic cholesterol esters robustly increased in both groups following WD (16- and 29-fold, respectively, *P* < 0.05), but were 32% higher in LCR than HCR rats after WD (interaction, *P* < 0.05).

We next examined expression of several genes (i.e. those for cholesterol metabolism, bile acid synthesis/steroidogenesis, and cholesterol/bile acid transporters) that may be responsible for strain or diet differences in liver cholesterol ester levels (Table 3). Several genes (e.g. *HMGCR*, *SOAT2*, *CYP7a1*, *HSD17b* and *ABCA1*) displayed significant changes in expression between the LCR and HCR rats following chronic WD (significant interactions, *P* < 0.05), implicating intrinsic aerobic capacity as a modulator of liver sterol homeostasis. These data show that while HCR and LCR rats both display

WD-induced steatosis, the LCR rats with reduced intrinsic aerobic capacity are much more susceptible to hepatic cholesterol ester storage and inflammatory cell infiltration.

### Liver inflammation

We next examined hepatic expression of genetic markers of white cell infiltration, recruitment/activation, and initiation/propagation of inflammatory signals. Liver mRNA expression of macrophage marker F4/80 was only increased in the WD-fed LCR rats (Fig. 2A, ~3-fold, interaction, *P* < 0.05). In addition, WD resulted in more dramatic increases in monocyte chemoattractant protein 1 (MCP-1), IL-1 $\beta$ , and the toll-like receptors 2, 4, and 9 (TLR2, 4 and 9) in LCR compared to HCR rats (Fig. 2B and C, significant interactions, *P* < 0.05). Hepatic expression of death receptors TRAIL2, Fas and TNFR1 were all increased in LCR WD compared to LFD and HCR WD rats (Fig. 2D, *P* < 0.05). Furthermore, significant WD-induced increases in liver inflammatory gene expression of NLRP3, TNFA, CD11c, CD68 and CD64 were observed in both strains

(Table 3), with no effects of strain observed. These data show that intrinsic aerobic capacity significantly alters susceptibility to WD-induced NASH outcomes.

### Liver fatty acid oxidation and acyl-carnitine profiles

We have previously shown that decreased intrinsic aerobic capacity is associated with reduced liver complete fatty acid oxidation (FAO) and more pronounced NAFLD outcomes (Rector *et al.* 2008; Thyfault *et al.* 2009; Morris *et al.* 2012, 2014, 2016). To further assess the role of

intrinsic aerobic capacity and chronic WD on liver lipid oxidation, we performed FAO experiments in liver homogenate and determined liver and plasma acyl-carnitine profiles. Chronic WD resulted in a ~45% reduction of complete FAO in both strains (Fig. 3A,  $P < 0.05$ ), with the HCR WD rats maintaining a 33% greater complete FAO to CO<sub>2</sub> compared to LCR rats ( $P < 0.05$ ). WD resulted in a significant decrease in acid-soluble metabolite (ASM) production in both strains (HCR, 6%; LCR, 18%;  $P < 0.05$ ), but a larger decrease in LCR than HCR rats (interaction,  $P < 0.05$ ). These changes were not due

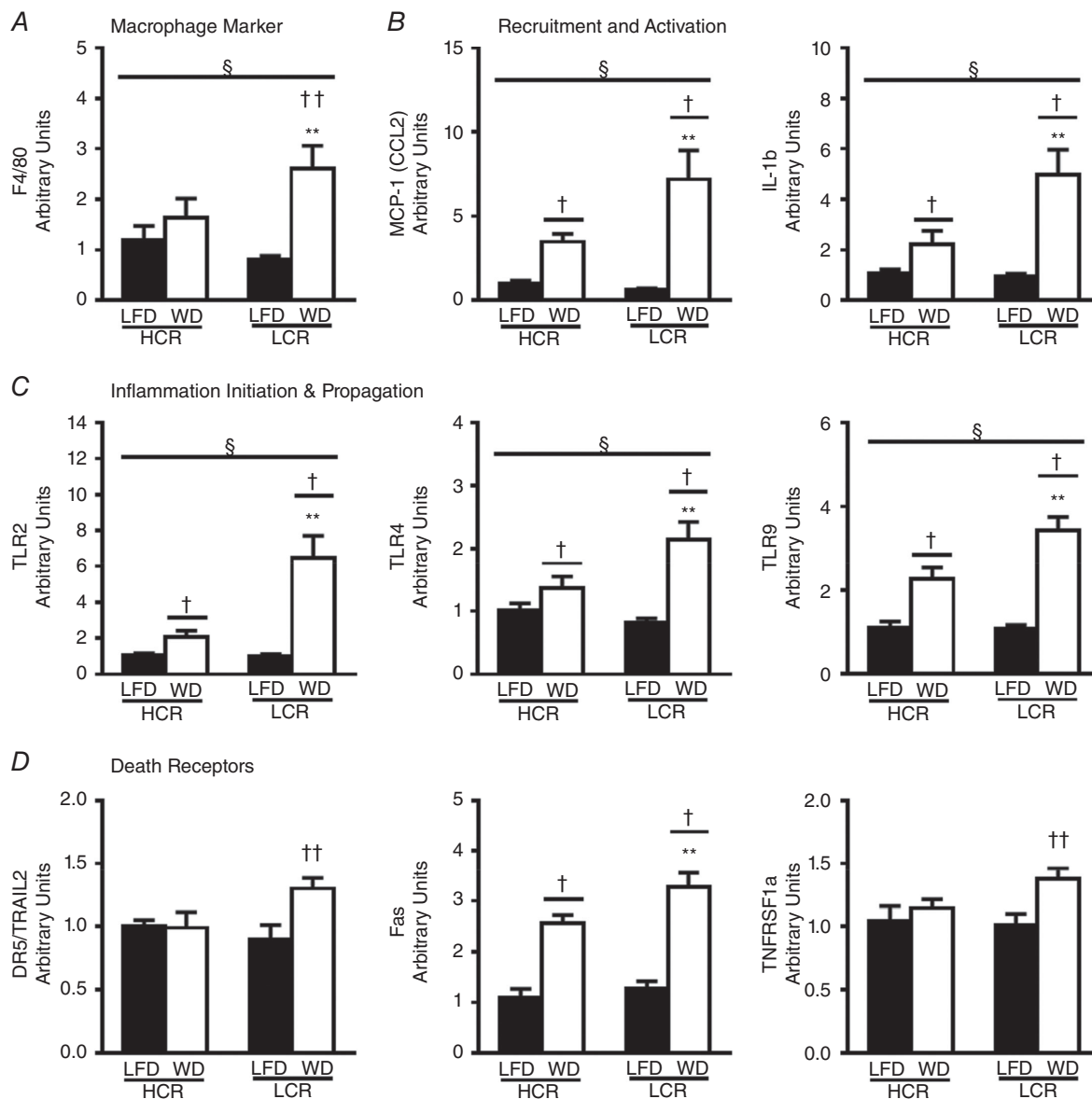


**Figure 2. High intrinsic aerobic capacity attenuates high-fat/high-cholesterol diet-induced expression of markers of liver macrophage infiltration and inflammation**

Gene expression in liver was determined by RT-PCR. Relative mRNA expression of genes for macrophage markers (A), recruitment and activation (B), inflammation initiation and propagation (C), and death receptors (D) were normalized to cyclophilin B (*PP1B*) and presented as means  $\pm$  SEM ( $n = 7-8$ ). § $P < 0.05$  interaction; \* $P < 0.05$  main effect HCR vs. LCR; † $P < 0.05$  main effect LFD vs. WD; \*\* $P < 0.05$  HCR vs. LCR within diet.



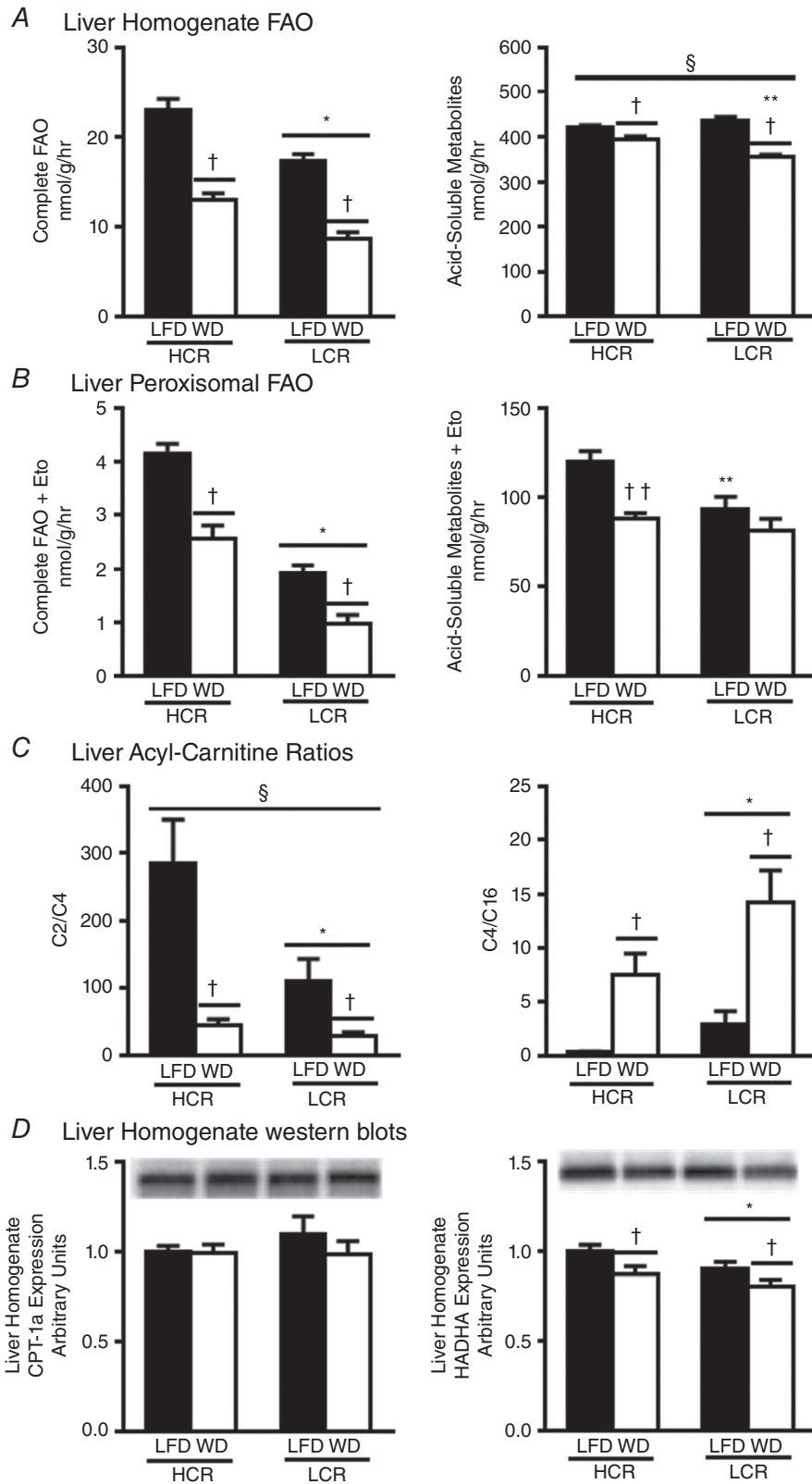


**Figure 3. Selection for increased running capacity results in greater hepatic fatty acid oxidation (FAO) and acyl-carnitine flux**

Liver homogenates were incubated with [ $^{14}$ C]palmitate. Complete FAO (A) was determined by trapping  $^{14}$ CO $_2$ , and acid-soluble metabolite (ASM) production was determined from the reaction buffer and normalized to liver sample wet weight. Parallel incubations of liver homogenate were performed in the presence of the CPT-1 inhibitor, etomoxir, to determine non-CPT-1-mediated (B) complete FAO and ASM production. Liver acyl-carnitine concentrations were determined by LC-MS/MS, and ratios (C) of C2/C4 and C4/C16 were compared to assess complete FAO and  $\beta$ -oxidation, respectively. (D) Western blot analysis of liver homogenate was performed to assess protein expression of CPT-1a and HADHA. Values are means  $\pm$  SEM ( $n = 8$ ).  $\S P < 0.05$  interaction;  $*P < 0.05$  main effect HCR vs. LCR;  $\dagger P < 0.05$  main effect LFD vs. WD;  $**P < 0.05$  HCR vs. LCR within diet;  $\dagger\dagger P < 0.05$  LFD vs. WD within strain.

to changes in protein expression of CPT-1a, (Fig. 3D). However, both complete FAO and ASM production appear to associate with total HADHA (trifunctional enzyme subunit a, mitochondria) protein expression, which was lower in the LCR rats on LFD and was reduced in both groups by the WD (Fig. 3D,  $P < 0.05$ ).

While up to 90% of liver FAO is localized to the mitochondria, the impact of increased peroxisomal  $\beta$ -oxidation on liver disease initiation and progression has not been extensively studied. To approximate peroxisomal FAO, liver homogenate FAO was determined in the presence of the CPT-1 inhibitor etomoxir. In the presences of etomoxir, the relative differences for all FAO data (Fig. 3B) strongly mirrored the absolute values above. Complete FAO due to peroxisomal oxidation was  $\sim 40\%$  higher in the HCR compared to LCR rats regardless of diet ( $P < 0.05$ ) and ASM production from peroxisomes was also higher in HCR rats on LFD ( $P < 0.05$ ). WD lowered peroxisomal ASM production only in the HCR but not the LCR rats ( $P < 0.05$ ). These data suggest that intrinsic aerobic capacity impacts liver peroxisomal FAO and may impact susceptibility for liver disease.

Acyl-carnitine profiling was performed in liver and plasma to further characterize the role of differing intrinsic aerobic capacity upon lipid metabolism, (Fig. 3C and Table 4). WD produced a significant decrease in the C2/C4 acyl-carnitine ratio compared to LFD ( $P < 0.05$ ) in both strains due to increases in C4-carnitine. However, the change in C2/C4 was significantly greater following WD in the HCR than the LCR rats (interaction,  $P < 0.05$ ). An opposite effect was observed for the C4/C16 acyl-carnitine ratio, where it was increased in both groups following WD, but was increased to a greater extent in the LCR rats ( $P < 0.05$ ). A decrease in the C2/C4 and an increase in the C4/C16 acyl-carnitine ratios suggest a decrease in complete fatty acid oxidation and/or an increase in  $\beta$ -oxidation leading to the subsequent accumulation of short-chain C4-carnitine. Additionally, liver long-chain (C14 and C16) acyl-carnitine levels were lower in the LCR compared to HCR rats, and were lowered in both strains following WD exposures ( $P < 0.05$ ). Further, medium-chain (C8) acyl-carnitines were lowered by WD in both strains ( $P < 0.05$ ). In addition to implicating increased liver  $\beta$ -oxidation of these species following chronic WD, the lower liver levels of medium- and long-chain acyl-carnitines also may suggest

greater diversion of excess liver acyl-CoAs toward the TAG synthesis pathway. This interpretation is supported by the gross steatosis observed in both strains on the WD. Hepatic free carnitine decreased following WD in both strains (Table 4,  $P < 0.05$ ), but the reduction was significantly greater in the LCR vs. HCR rats (interaction,  $P < 0.05$ ). WD diet caused an equal increase in plasma free carnitine in both strains suggesting that hepatic tissue metabolism following WD was different between strains. Plasma and liver C2-carnitine patterns were similar in the HCR rats on both diets but the WD significantly decreased liver C2-carnitine in the LCR rats. All told, these data demonstrate that reduced intrinsic aerobic capacity is associated with decreased hepatic FAO and FAO adaptability to the WD challenge.

#### Liver mitochondrial content, respiration and energy state

Reductions in hepatic mitochondrial number, mitochondrial respiratory capacity (MRC), and energy state have also been implicated in the development of NAFLD (Begrache *et al.* 2013; Arguello *et al.* 2015). Hepatic mitochondrial content, assessed by citrate synthase activity, was reduced 23% by WD in both strains (Fig. 4A,  $P < 0.05$ ); however, content remained 16% higher in the HCR than LCR rats ( $P < 0.05$ ). We previously reported (Morris *et al.* 2014, 2016) evidence of reduced liver mitochondria TCA cycle flux (measured by 2- $^{14}$ C]pyruvate oxidation) combined with reduced MRC in LCR rats. Here we report that WD lowered 2- $^{14}$ C]pyruvate oxidation in isolated mitochondria to a greater extent in the LCR vs. HCR rats (69% vs. 28%, respectively; Fig. 4A,  $P < 0.05$ ). Similarly, WD feeding reduced ADP-stimulated mitochondrial respiration of glutamate through complex I and complex I and II to a greater extent in LCR vs. HCR rats (Fig. 4B,  $P < 0.05$ ), whereas, maximal uncoupled mitochondrial respiration of glutamate was significantly increased following WD feeding in HCR compared with LCR rats (Fig. 4B,  $P < 0.05$ ). Mitochondrial respiration experiments with pyruvate and palmitoyl-carnitine produced similar findings (data not shown).

Because of differences in hepatic FAO and MRC, we also measured hepatic energy status (NAD and adenine nucleotide pools). LCR rats displayed greater NADH than

**Table 4. Plasma and liver acyl-carnitine profiles**

	HCR		LCR		Interaction
	LFD	WD	LFD	WD	
<b>Serum (<math>\mu\text{M}</math>)</b>					
Free carnitine	40.64 $\pm$ 2.85	49.87 $\pm$ 2.49 <sup>††</sup>	55.31 $\pm$ 2.64*	57.93 $\pm$ 2.38*	NS
Acetyl-carnitine (C2)	27.77 $\pm$ 2.26	29.88 $\pm$ 1.58	39.63 $\pm$ 3.07*	36.53 $\pm$ 2.21*	NS
Isopropyl-carnitine (C3)	0.1532 $\pm$ 0.0150	0.2467 $\pm$ 0.0122 <sup>†</sup>	0.2207 $\pm$ 0.0143*	0.3662 $\pm$ 0.0132*, <sup>†</sup>	$P < 0.07$
Butyryl-carnitine (C4)	0.2962 $\pm$ 0.0245	0.3218 $\pm$ 0.0463	0.4153 $\pm$ 0.0195*	0.4610 $\pm$ 0.0492*	NS
Isovaleryl-carnitine (C5)	0.0112 $\pm$ 0.0021	0.0107 $\pm$ 0.0003	0.0113 $\pm$ 0.0007	0.0127 $\pm$ 0.0006	NS
Octanoyl-carnitine (C8)	0.0139 $\pm$ 0.0007	0.0126 $\pm$ 0.0004	0.0134 $\pm$ 0.0004	0.0137 $\pm$ 0.0006	NS
Mistroyl-carnitine (C14)	0.0546 $\pm$ 0.0041	0.0491 $\pm$ 0.0038	0.0555 $\pm$ 0.0027	0.0424 $\pm$ 0.0017 <sup>††</sup>	NS
Palmitoyl-carnitine (C16)	0.3358 $\pm$ 0.0488	0.3361 $\pm$ 0.0400	0.3652 $\pm$ 0.0267	0.3138 $\pm$ 0.0215	NS
<b>Liver (nmol g<sup>-1</sup>)</b>					
Free carnitine	304.2 $\pm$ 10.9	209.3 $\pm$ 23.2 <sup>†</sup>	335.9 $\pm$ 7.2*	123.6 $\pm$ 7.9*, <sup>†</sup>	$P < 0.001$
Acetyl-carnitine (C2)	105.7 $\pm$ 10.2	109.3 $\pm$ 9	99.4 $\pm$ 11.2	110.3 $\pm$ 8.2	NS
Isopropyl-carnitine (C3)	3.22 $\pm$ 0.74	3.91 $\pm$ 0.36	1.72 $\pm$ 0.18**	3.09 $\pm$ 0.36 <sup>††</sup>	NS
Butyryl-carnitine (C4)	0.650 $\pm$ 0.230	3.119 $\pm$ 0.611 <sup>†</sup>	1.315 $\pm$ 0.362	5.048 $\pm$ 1.370 <sup>†</sup>	NS
Isovaleryl-carnitine (C5)	0.1321 $\pm$ 0.0190	0.1566 $\pm$ 0.217	0.1434 $\pm$ 0.0123	0.1052 $\pm$ 0.181	NS
Octanoyl-carnitine (C8)	0.0592 $\pm$ 0.0106	0.0226 $\pm$ 0.0052 <sup>†</sup>	0.0555 $\pm$ 0.0110	0.0151 $\pm$ 0.0014 <sup>†</sup>	NS
Mistroyl-carnitine (C14)	1.250 $\pm$ 0.232	0.216 $\pm$ 0.061 <sup>†</sup>	0.676 $\pm$ 0.142**	0.213 $\pm$ 0.049 <sup>†</sup>	$P < 0.07$
Palmitoyl-carnitine (C16)	1.185 $\pm$ 0.187	0.490 $\pm$ 0.133 <sup>†</sup>	0.671 $\pm$ 0.136*	0.266 $\pm$ 0.030*, <sup>†</sup>	NS
<b>Liver carnitine ratios</b>					
C2/C3	48.4 $\pm$ 7.9	29.2 $\pm$ 3.2 <sup>†</sup>	52.8 $\pm$ 4.6	37.5 $\pm$ 2.9 <sup>†</sup>	NS
C2/C4	285.2 $\pm$ 65.0	44.5 $\pm$ 9.6 <sup>†</sup>	110.3 $\pm$ 33.1*	30.3 $\pm$ 5.0*, <sup>†</sup>	$P < 0.05$
C4/C16	0.312 $\pm$ 0.078	7.480 $\pm$ 2.022 <sup>†</sup>	2.929 $\pm$ 1.230*	14.276 $\pm$ 2.894*, <sup>†</sup>	NS
C8/C16	0.039 $\pm$ 0.006	0.033 $\pm$ 0.004	0.091 $\pm$ 0.012*	0.066 $\pm$ 0.007*, <sup>††</sup>	NS

Plasma and liver acyl-carnitines were quantitated by LC-MS/MS. Liver acyl-carnitines were normalized to liver samples weight. All values are presented as means  $\pm$  SEM ( $n = 7-8$ ).  $P < 0.05$  interaction; \* $P < 0.05$  main effect HCR vs. LCR; <sup>†</sup> $P < 0.05$  main effect LFD vs. WD; \*\* $P < 0.05$  HCR vs. LCR within diet; <sup>††</sup> $P < 0.05$  LFD vs. WD within strain. NS, not significant.

HCR rats on LFD (Table 5,  $P < 0.05$ ). WD significantly reduced NAD<sup>+</sup>, NADH, total NAD, AMP, ADP, ATP and total nucleotides in both strains ( $P < 0.05$ ). To reduce the impact of WD-induced hepatomegaly on the interpretation of these findings, we calculated within liver sample NAD<sup>+</sup>/NADH ratio and adenine energy state. Interestingly, no difference due to strain or diet was observed in hepatic energy charge as calculated from adenine nucleotides (Fig. 4C). WD significantly lowered NAD<sup>+</sup>/NADH in both strains ( $P < 0.05$ ). Importantly, the greater NADH of the LCR rats (Table 5) resulted in a lower liver NAD<sup>+</sup>/NADH ratio compared to HCR rats on both diets (Fig. 4C,  $P < 0.05$ ). Chronically reduced NAD<sup>+</sup>/NADH within the LCR rats is suggestive of greater oxidative stress (Fisher-Wellman & Neuffer, 2012), which was further supported by higher hepatic lipid peroxidation (4-HNE) and evidence of hydrogen peroxide handling (GPx1) in the LCR over HCR rats (Fig. 5,  $P < 0.05$ ). In total, these data show that low intrinsic aerobic capacity tracks with reduced liver mitochondrial content, TCA cycle flux and respiratory capacity that is worsened with a WD. In addition, low-fitness LCR rats displayed a more reduced oxidative state, particularly following chronic WD feeding.

### Liver mitochondrial integrity and effector caspase activation

Mitochondria serve as a primary cellular site for regulation and integration of intra- and extracellular signals modulating inflammatory and cell death signalling (Guicciardi *et al.* 2013). We measured hepatic mitochondrial specific content of Bcl-2 family proteins involved in regulating mitochondrial outer membrane permeability (MOMP) and downstream effector caspases to assess the impact of divergent aerobic capacity and WD on these portions of the cell death cascade. Mitochondrial content of the anti-apoptotic protein Bcl-2 was increased, while Bcl-xL was decreased by WD in both strains (Fig. 6A,  $P < 0.05$ ). Pro-apoptotic Bcl-2 family members, Bax, Bak and cleaved Bcl-xL, were all significantly increased following WD in both strains (Fig. 6B,  $P < 0.05$ ). Interestingly, cleaved Bcl-xL mitochondrial localization was greater in LCR rats on both LFD and WD (29% and 39%, respectively) compared to HCR rats.

To assess whether these elevated markers of mitochondrial outer membrane permeability were associated with activation of downstream pathways, caspase 3 and 7 protein activation status was determined (Fig. 6C). Both

caspace 3 and 7 showed greater activation in the LCR compared to HCR rats regardless of diet (~60% and 4-fold, respectively,  $P < 0.05$ ). WD increased activation of caspace 3 but not 7 in HCR and LCR rats (39% and 48%, respectively,  $P < 0.05$ ). Thus, WD-induced changes in hepatic mitochondrial integrity between rats with divergent intrinsic aerobic capacities do not result in similarly associated changes in caspace activation. Further,

selection for low aerobic capacity is associated with greater basal activation of hepatic effector caspases, which is exacerbated by chronic WD feeding.

## Discussion

Despite numerous findings in humans that aerobic capacity impacts liver disease progression, mechanisms

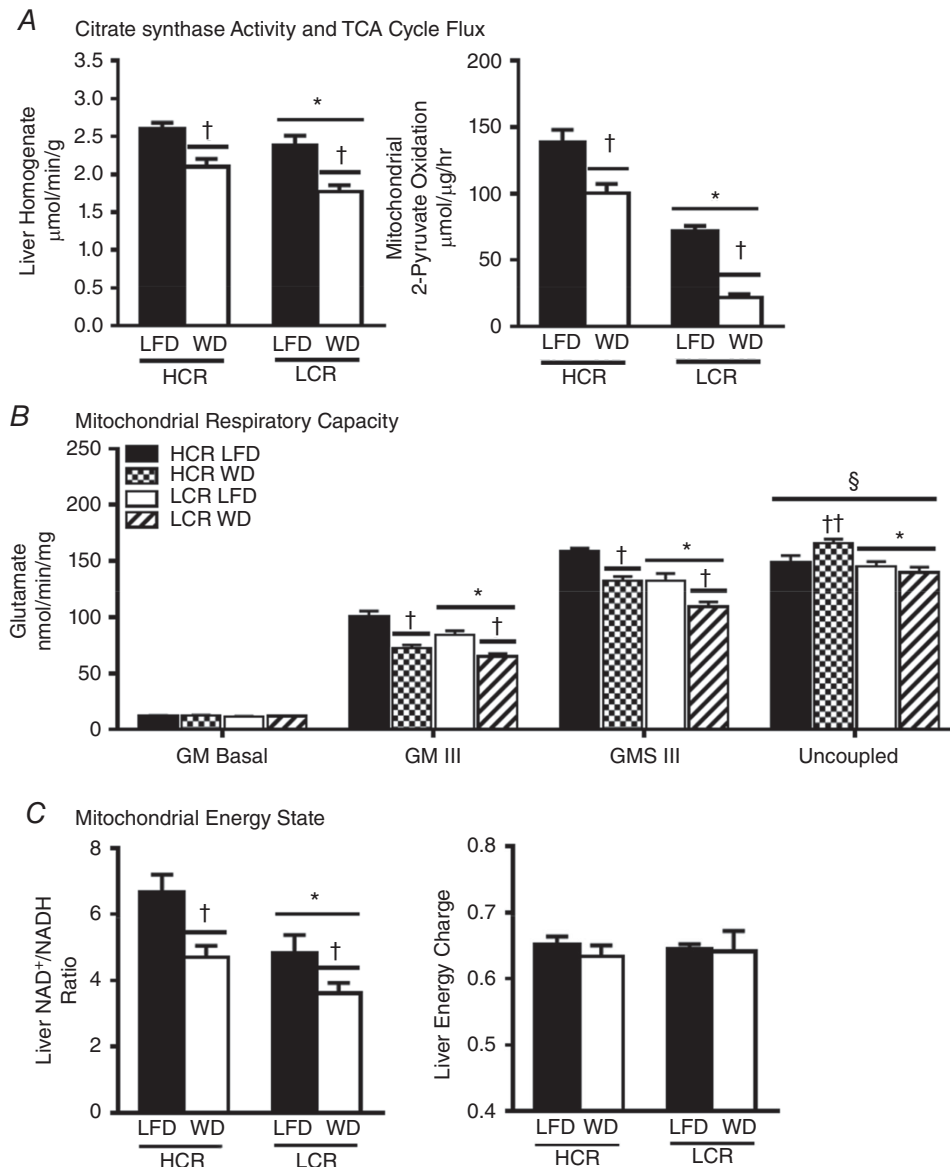


**Figure 4. Liver mitochondrial content, respiratory capacity and hepatic NAD<sup>+</sup>/NADH ratio is higher in rats with high intrinsic aerobic capacity**

A, markers of hepatic mitochondrial content and TCA cycle flux are presented as citrate synthase activity in liver homogenate and 2-[<sup>14</sup>C]pyruvate oxidation to CO<sub>2</sub>. B, liver mitochondrial respiration was determined by measurement of O<sub>2</sub> consumption using a Clark electrode system in the presence of glutamate (+malate and succinate) in different respiratory states (basal, state 3 and uncoupled). C, hepatic NAD<sup>+</sup>, NADH, ATP, ADP, and AMP were determined by LC-MS/MS. The mitochondrial energy state is represented as the ratio of NAD<sup>+</sup> to NADH, and adenine energy charge. Values are means  $\pm$  SEM ( $n = 7-8$ ).  $\S P < 0.05$  interaction;  $*P < 0.05$  main effect HCR vs. LCR;  $\dagger P < 0.05$  main effect LFD vs. WD;  $\dagger\dagger P < 0.05$  LFD vs. WD within strain.

**Table 5. Liver NAD and adenine nucleotides**

	HCR		LCR		Interaction
	LFD	WD	LFD	WD	
<b>NAD pool (nmol g<sup>-1</sup>)</b>					
NAD <sup>+</sup>	1022.6 ± 40.3	641.0 ± 31.3 <sup>†</sup>	1078.4 ± 84.6	553.0 ± 44.7 <sup>†</sup>	NS
NADH	158.8 ± 10.0	130.6 ± 8.1 <sup>†</sup>	239.7 ± 28.6*	158.4 ± 9.2*, <sup>†</sup>	<i>P</i> = 0.06
Total NAD	1181.5 ± 38.1	783.9 ± 40.4 <sup>†</sup>	1318.1 ± 101.7*	711.3 ± 42.9*, <sup>†</sup>	<i>P</i> = 0.06
<b>Adenine nucleotide pool (nmol g<sup>-1</sup>)</b>					
AMP	855.2 ± 42.4	663.9 ± 72.4 <sup>†</sup>	938.1 ± 64.9	581.8 ± 70.6 <sup>†</sup>	NS
ADP	1549.7 ± 90.2	1220.7 ± 101.9 <sup>†</sup>	1863.9 ± 137.7	1186.2 ± 111.7 <sup>†</sup>	NS
ATP	2254.2 ± 76.2	1553.7 ± 82.3 <sup>†</sup>	2467.0 ± 117.6	1739.8 ± 180.6 <sup>†</sup>	NS
Total adenine pool	4659.1 ± 124.8	3438.3 ± 217.5 <sup>†</sup>	5429.2 ± 376.8	3507.8 ± 242.5 <sup>†</sup>	NS

Chronic high-fat/high-cholesterol diet lowers liver adenine nucleotides in HCR/LCR rats. Liver adenine nucleotide (NAD<sup>+</sup>, NADH, AMP, ADP, and ATP) quantitation was determined by LC-MS/MS and all values were normalized to liver sample weight. All values are presented as means ± SEM (*n* = 7–8). *P* < 0.05 interaction; \**P* < 0.05 main effect HCR vs. LCR; <sup>†</sup>*P* < 0.05 main effect LFD vs. WD; \*\**P* < 0.05 HCR vs. LCR within diet; <sup>††</sup>*P* < 0.05 LFD vs. WD within strain.

remain unknown. Likewise, factors that drive transition from NAFLD to NASH in only a proportion of patients remain unknown. Here, we find low aerobic fitness and reduced initial hepatic mitochondrial oxidative capacity enhance susceptibility to WD-induced NASH, as characterized by increased serum ALT, inflammatory cell infiltration, effector caspase activation, and mRNA expression of pro-inflammatory and cell death signalling genes. Importantly, evidence of trans-

ition to NASH was only found in the low-fitness LCR rats despite both high-fitness HCR and low-fitness LCR rats developing robust hepatomegaly and steatosis. Overall, the data show that intrinsic aerobic capacity and hepatic mitochondrial oxidative capacity impact cholesterol ester accumulation and inflammatory status following WD, and support the concept that these physiological factors drive risk for transition from NAFLD to NASH.

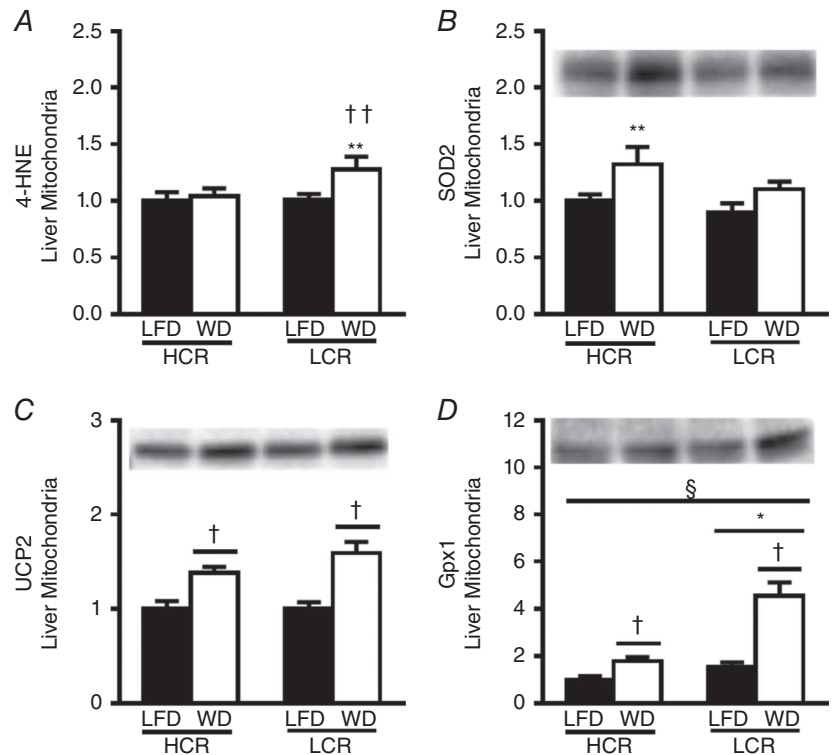


**Figure 5. Protein expression of markers of oxidative stress and anti-oxidant enzymes in isolated liver mitochondria**

Data are presented as means ± SEM (*n* = 7–8). A, 4-hydroxy-2-nonenal (4-HNE); B, superoxide dismutase 2 (SOD2); C, uncoupling protein 2 (UCP2); D, glutathione peroxidase 1 (GPx1). §*P* < 0.05 interaction; \**P* < 0.05 main effect HCR vs. LCR; <sup>†</sup>*P* < 0.05 main effect LFD vs. WD; \*\**P* < 0.05 HCR vs. LCR within diet; <sup>††</sup>*P* < 0.05 LFD vs. WD within strain.

The roles of both maladaptive liver cholesterol metabolism and hepatic mitochondrial function have been widely investigated in the development of NAFLD (Min *et al.* 2012; Arguello *et al.* 2015; Bashiri *et al.* 2016). Excess dietary cholesterol results in hepatomegaly and steatosis, reduced liver complete and total FAO, and decreased

ADP-coupled mitochondrial respiration in rats (Rogers *et al.* 1980; Fungwe *et al.* 1993), while chemical inhibition of endogenous cholesterol synthesis increased hepatic mitochondrial and peroxisomal FAO with protection from NASH development (Roglans *et al.* 2002; Park *et al.* 2016). In the current study, WD reduced FAO (complete and

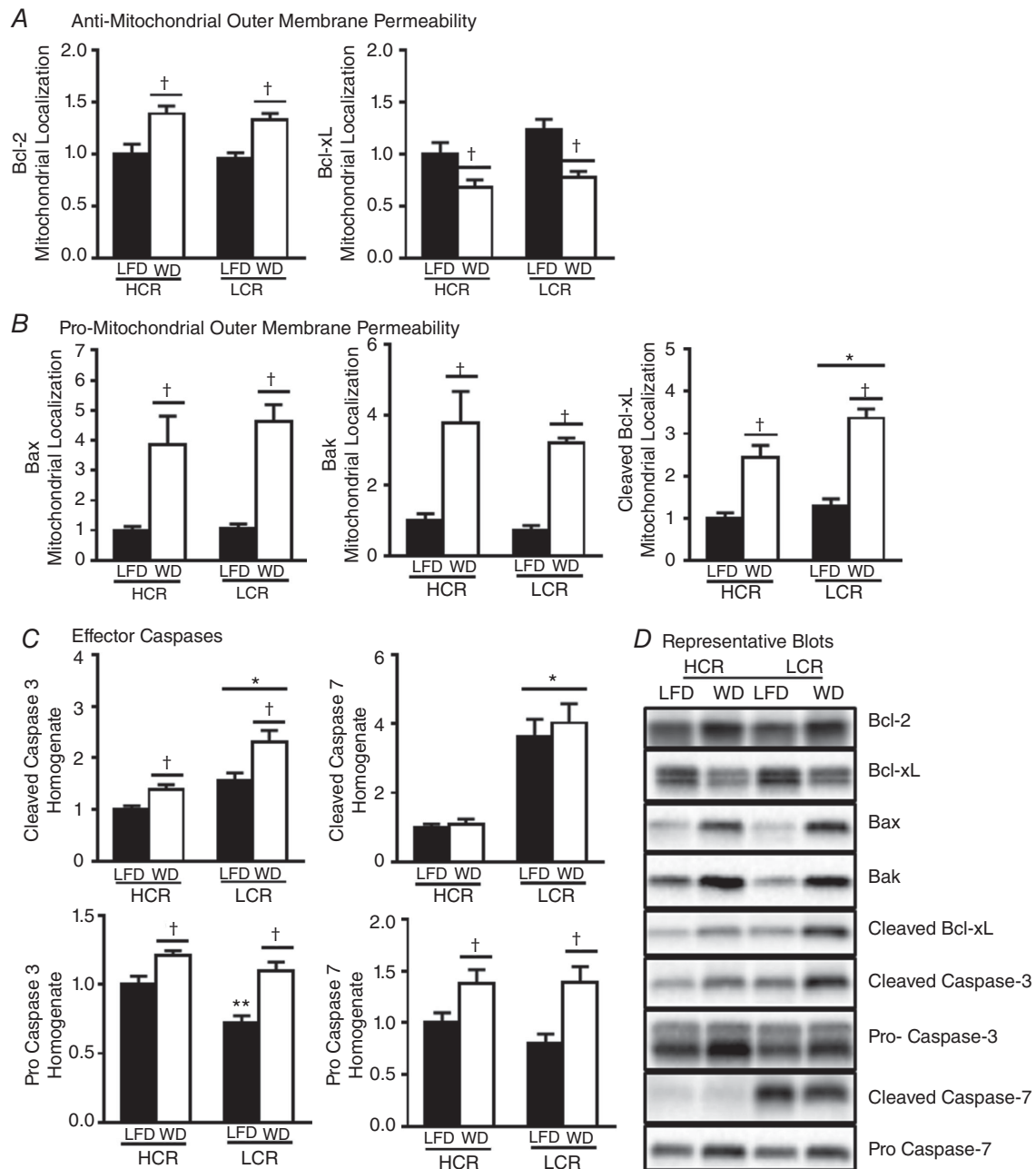


**Figure 6. Low intrinsic aerobic capacity increases susceptibility to liver mitochondrial localization of pro-apoptotic proteins and associated effector caspase activation**

A and B, mitochondrial localization of proteins involved in the regulation of mitochondrial outer membrane permeability (MOMP) were determined in isolated liver mitochondria by Western blot analysis. A, anti-MOMP opening (Bcl-2 and Bcl-xL). B, pro-MOMP opening (Bax, Bak and cleaved BCL-xL). C, liver expression of active (cleaved) effector caspases, caspase-3 and caspase-7, was determined in liver homogenate by Western blot analysis. D, representative blots. All values are presented as means  $\pm$  SEM ( $n = 7-8$ ). \* $P < 0.05$  main effect HCR vs. LCR, †  $P < 0.05$  main effect LFD vs. WD, \*\*  $P < 0.05$  HCR vs. LCR within diet.

incomplete) and MRC in both strains, but the LCR rats started at a lower level and remained lower than HCR rats. In addition, the impact of the lower levels of FAO and MRC in isolated mitochondria is further magnified by the overall lower mitochondrial content in the LCR vs. HCR rats. Similar findings were observed with markers of liver mitochondrial content, TCA cycle flux and free hepatic carnitine content. We have previously observed that LCR rats have increased susceptibility to steatosis, which was associated with reduced whole body FAO, metabolic inflexibility, decreased liver FAO and reduced MRC (Thyfault *et al.* 2009; Morris *et al.* 2014, 2016). These data are similar to human NAFLD subjects who have been shown to have physiological features that include lower aerobic capacity, metabolic inflexibility, decreased whole body FAO, and reduced  $\beta$ -hydroxybutyrate, all factors that suggest reduced liver FAO capacity (Crocini *et al.* 2012). Additional rodent studies have demonstrated that reduced hepatic complete FAO is associated with development and progression of hepatic steatosis (Rector *et al.* 2008, 2010) while molecular therapies to enhance FAO effectively treat or prevent steatosis. Importantly, our findings of greater WD-induced reductions in mitochondrial FAO and MRC in LCR rats appear to be independent of TAG accumulation, suggesting that hepatic TAG stores are not the primary driver of inflammation and oxidative stress, but rather that hepatic mitochondrial function plays a more important role. These results are similar to the athletes' paradox by which both athletes and insulin-resistant obese individuals display dramatically different insulin sensitivity and inflammation despite both displaying elevated intramuscular lipids (Goodpaster *et al.* 2001). Much like in muscle, it is possible that the overall balance of hepatic mitochondrial content/oxidative capacity and lipid stores interact to impact outcomes related to inflammation and insulin resistance.

Mitochondria are hypothesized to serve as a cellular point of integration of intra- and extracellular signals ultimately producing inflammation and cell death signalling (Guicciardi *et al.* 2013; Luedde *et al.* 2014; Arguello *et al.* 2015). Dysregulated liver cholesterol homeostasis and accumulation has been implicated in the initiation of hepatic mitochondrial dysfunction (Montero *et al.* 2010), which is associated with NAFLD severity (Min *et al.* 2012). Mitochondrial membranes are inherently cholesterol poor (Montero *et al.* 2010), with increased mitochondrial membrane cholesterol producing decreased ATP synthesis (Campbell & Chan, 2007) and decreased mitochondrial antioxidant capacity (Fernandez-Checa & Kaplowitz, 2005). In the present study, maximal ADP-coupled MRC was lowered to a greater extent following WD in the LCR rats, results that tracked with greater induction of mitochondrial oxidative stress. Previously, increased free cholesterol levels were highly associated with NASH-related mitochondrial

dysfunction (Min *et al.* 2012; Gan *et al.* 2014). Interestingly, here the reductions in MRC and increased markers of oxidative stress occurred in parallel with an observed increase in cholesterol ester in LCR compared to HCR rats on the WD. Chronic accumulation of mitochondrial cholesterol is associated with increased mitochondrial localization of pro-apoptotic Bcl-2 family members and activation of MOMP (Montero *et al.* 2010). Chronic WD feeding in this study resulted in similar increases in mitochondrial protein localization of Bax and Bak in both strains, while lowering the predominant liver anti-MOMP Bcl family member, Bcl-xL. Mitochondrial localization of the pro-apoptotic Bcl-xL cleavage product (Clem *et al.* 1998; Fujita *et al.* 1998) was significantly higher in the WD-fed LCR rats compared to HCR rats, and was strongly associated with the observed increases in markers of advance NAFLD.

We found that effector caspase activation was higher in LCR compared to HCR rats regardless of diet, with WD dramatically increasing caspase-3 activation further. This increase in caspase-3 activation could potentially explain the observed increase in cleaved Bcl-xL (Clem *et al.* 1998; Fujita *et al.* 1998). The increased effector caspase activation also suggests greater intrinsic/extrinsic cell death signalling in the LCR on WD, which is further supported by the observed increases in cell death receptor expression. As mentioned, there is considerable evidence that loss of mitochondrial function and excess cholesterol can result in propagation of these intrinsic/extrinsic cell death signals (Guicciardi *et al.* 2013; Luedde *et al.* 2014; Arguello *et al.* 2015). However, any increased cell death signalling in the LCR rats on WD is early in the disease process as assessment of cell death by TUNEL assay showed no differences between HCR and LCR rats (data not shown). Together, these data suggest that intrinsically low aerobic capacity results in increased susceptibility to WD-induced steatohepatitis due to lower mitochondrial respiratory capacity, increased oxidative stress and greater activation of effector caspases.

In summary, we demonstrate that intrinsic aerobic capacity impacts susceptibility for WD-induced NASH. Lower initial levels and further declines in liver FAO and MRC paired with excessive liver cholesterol ester accumulation lead to greater increases in several markers of liver damage and inflammation in the low-fitness LCR compared to the high-fitness HCR rats. Of note, while high intrinsic aerobic capacity HCR rats were less susceptible to many of the liver mal-adaptations induced by a WD, HCR rats were not completely protected against hepatomegaly/liver TAG accumulation or against a loss of mitochondrial FAO or MRC unlike our previous findings with acute and chronic high-fat diets (Thyfault *et al.* 2009; Morris *et al.* 2014, 2016). These data support a novel concept that aerobic capacity and hepatic mitochondrial phenotype may play a critical role

in whether NAFLD transitions to NASH, links that require further examination in human patients. Overall, these data provide new insight into how intrinsic aerobic capacity may influence the onset and progression of metabolic disease through hepatic mitochondrial oxidative capacity.

## References

- Arguello G, Balboa E, Arrese M & Zanlungo S (2015). Recent insights on the role of cholesterol in non-alcoholic fatty liver disease. *Biochim Biophys Acta* **1852**, 1765–1778.
- Bashiri A, Nesan D, Tavallae G, Sue-Chue-Lam I, Chien K, Maguire GF, Naples M, Zhang J, Magomedova L, Adeli K, Cummins CL & Ng DS (2016). Cellular cholesterol accumulation modulates high fat high sucrose (HFHS) diet-induced ER stress and hepatic inflammasome activation in the development of non-alcoholic steatohepatitis. *Biochim Biophys Acta* **1861**, 594–605.
- Begriffe K, Massart J, Robin MA, Bonnet F & Fromenty B (2013). Mitochondrial adaptations and dysfunctions in nonalcoholic fatty liver disease. *Hepatology* **58**, 1497–1507.
- Bernal W, Martin-Mateos R, Lipcsey M, Tallis C, Woodsford K, McPhail MJ, Willars C, Auzinger G, Sizer E, Heneghan M, Cottam S, Heaton N & Wendon J (2014). Aerobic capacity during cardiopulmonary exercise testing and survival with and without liver transplantation for patients with chronic liver disease. *Liver Transpl* **20**, 54–62.
- Campbell AM & Chan SH (2007). The voltage dependent anion channel affects mitochondrial cholesterol distribution and function. *Arch Biochem Biophys* **466**, 203–210.
- Church TS, Kuk JL, Ross R, Priest EL, Biltoft E & Blair SN (2006). Association of cardiorespiratory fitness, body mass index, and waist circumference to nonalcoholic fatty liver disease. *Gastroenterology* **130**, 2023–2030.
- Clem RJ, Cheng EH, Karp CL, Kirsch DG, Ueno K, Takahashi A, Kastan MB, Griffin DE, Earnshaw WC, Veluona MA & Hardwick JM (1998). Modulation of cell death by Bcl-XL through caspase interaction. *Proc Natl Acad Sci USA* **95**, 554–559.
- Croci I, Byrne NM, Choquette S, Hills AP, Chachay VS, Clouston AD, O'Moore-Sullivan TM, Macdonald GA, Prins JB & Hickman IJ (2012). Whole-body substrate metabolism is associated with disease severity in patients with non-alcoholic fatty liver disease. *Gut* **62**, 1625–1633.
- Fernandez-Checa JC & Kaplowitz N (2005). Hepatic mitochondrial glutathione: transport and role in disease and toxicity. *Toxicol Appl Pharmacol* **204**, 263–273.
- Fisher-Wellman KH & Neuffer PD (2012). Linking mitochondrial bioenergetics to insulin resistance via redox biology. *Trends Endocrinol Metab* **23**, 142–153.
- Fujita N, Nagahashi A, Nagashima K, Rokudai S & Tsuruo T (1998). Acceleration of apoptotic cell death after the cleavage of Bcl-XL protein by caspase-3-like proteases. *Oncogene* **17**, 1295–1304.
- Fungwe TV, Cagen LM, Cook GA, Wilcox HG & Heimberg M (1993). Dietary cholesterol stimulates hepatic biosynthesis of triglyceride and reduces oxidation of fatty acids in the rat. *J Lipid Res* **34**, 933–941.
- Gan LT, Van Rooyen DM, Koina ME, McCuskey RS, Teoh NC & Farrell GC (2014). Hepatocyte free cholesterol lipotoxicity results from JNK1-mediated mitochondrial injury and is HMGB1 and TLR4-dependent. *J Hepatol* **61**, 1376–1384.
- Gavini CK, Mukherjee S, Shukla C, Britton SL, Koch LG, Shi H & Novak CM (2014). Leanness and heightened non-resting energy expenditure: role of skeletal muscle activity thermogenesis. *Am J Physiol Endocrinol Metab* **306**, E635–E647.
- Goodpaster BH, He J, Watkins S & Kelley DE (2001). Skeletal muscle lipid content and insulin resistance: evidence for a paradox in endurance-trained athletes. *J Clin Endocrinol Metab* **86**, 5755–5761.
- Guicciardi ME, Malhi H, Mott JL & Gores GJ (2013). Apoptosis and necrosis in the liver. *Compr Physiol* **3**, 977–1010.
- Kantartzis K, Thamer C, Peter A, Machann J, Schick F, Schraml C, Konigsrainer A, Konigsrainer I, Krober S, Niess A, Fritsche A, Haring HU & Stefan N (2009). High cardiorespiratory fitness is an independent predictor of the reduction in liver fat during a lifestyle intervention in non-alcoholic fatty liver disease. *Gut* **58**, 1281–1288.
- Koch LG & Britton SL (2001). Artificial selection for intrinsic aerobic endurance running capacity in rats. *Physiol Genomics* **5**, 45–52.
- Linden MA, Sheldon RD, Meers GM, Ortinau LC, Morris EM, Booth FW, Kanaley JA, Vieira-Potter VJ, Sowers JR, Ibdah JA, Thyfault JP, Laughlin MH & Rector RS (2016). Aerobic exercise training in the treatment of NAFLD related fibrosis. *J Physiol* **594**, 5271–5284.
- Luedde T, Kaplowitz N & Schwabe RF (2014). Cell death and cell death responses in liver disease: mechanisms and clinical relevance. *Gastroenterology* **147**, 765–783.e4.
- Matteoni CA, Younossi ZM, Gramlich T, Boparai N, Liu YC & McCullough AJ (1999). Nonalcoholic fatty liver disease: a spectrum of clinical and pathological severity. *Gastroenterology* **116**, 1413–1419.
- Min HK, Kapoor A, Fuchs M, Mirshahi F, Zhou H, Maher J, Kellum J, Warnick R, Contos MJ & Sanyal AJ (2012). Increased hepatic synthesis and dysregulation of cholesterol metabolism is associated with the severity of nonalcoholic fatty liver disease. *Cell Metab* **15**, 665–674.
- Montero J, Mari M, Colell A, Morales A, Basanez G, Garcia-Ruiz C & Fernandez-Checa JC (2010). Cholesterol and peroxidized cardiolipin in mitochondrial membrane properties, permeabilization and cell death. *Biochim Biophys Acta* **1797**, 1217–1224.
- Morris EM, Jackman MR, Johnson GC, Liu TW, Lopez JL, Kearney ML, Fletcher JA, Meers GM, Koch LG, Britton SL, Rector RS, Ibdah JA, MacLean PS & Thyfault JP (2014). Intrinsic aerobic capacity impacts susceptibility to acute high-fat diet-induced hepatic steatosis. *Am J Physiol Endocrinol Metab* **307**, E355–E364.
- Morris EM, Jackman MR, Meers GM, Johnson GC, Lopez JL, Maclean PS & Thyfault JP (2013). Reduced hepatic mitochondrial respiration following acute high-fat diet is prevented by PGC-1 $\alpha$  overexpression. *Am J Physiol Gastrointest Liver Physiol* **305**, G868–G880.



- Morris EM, Meers GM, Booth FW, Fritsche KL, Hardin CD, Thyfault JP & Ibdah JA (2012). PGC-1 $\alpha$  overexpression results in increased hepatic fatty acid oxidation with reduced triacylglycerol accumulation and secretion. *Am J Physiol Gastrointest Liver Physiol* **303**, G979–G992.
- Morris EM, Meers GM, Koch LG, Britton SL, Fletcher JA, Shankar K, Fu X, Burgess SC, Ibdah JA, Rector RS & Thyfault JP (2016). Aerobic capacity and hepatic mitochondrial lipid oxidation alters susceptibility for chronic high fat diet induced hepatic steatosis. *Am J Physiol Endocrinol Metab* **311**, E749–E760.
- Musso G, Gambino R, De Micheli F, Cassader M, Rizzetto M, Durazzo M, Faga E, Silli B & Pagano G (2003). Dietary habits and their relations to insulin resistance and postprandial lipemia in nonalcoholic steatohepatitis. *Hepatology* **37**, 909–916.
- Myers J, Prakash M, Froelicher V, Do D, Partington S & Atwood JE (2002). Exercise capacity and mortality among men referred for exercise testing. *N Engl J Med* **346**, 793–801.
- Noland RC, Thyfault JP, Henes ST, Whitfield BR, Woodlief TL, Evans JR, Lust JA, Britton SL, Koch LG, Dudek RW, Dohm GL, Cortright RN & Lust RM (2007). Artificial selection for high-capacity endurance running is protective against high-fat diet-induced insulin resistance. *Am J Physiol Endocrinol Metab* **293**, E31–E41.
- Novak CM, Escande C, Burghardt PR, Zhang M, Barbosa MT, Chini EN, Britton SL, Koch LG, Akil H & Levine JA (2010). Spontaneous activity, economy of activity, and resistance to diet-induced obesity in rats bred for high intrinsic aerobic capacity. *Horm Behav* **58**, 355–367.
- Park HS, Jang JE, Ko MS, Woo SH, Kim BJ, Kim HS, Park HS, Park IS, Koh EH & Lee KU (2016). Statins increase mitochondrial and peroxisomal fatty acid oxidation in the liver and prevent non-alcoholic steatohepatitis in mice. *Diabetes Metab J* **40**, 376–385.
- Rector RS, Thyfault JP, Morris RT, Laye MJ, Borengasser SJ, Booth FW & Ibdah JA (2008). Daily exercise increases hepatic fatty acid oxidation and prevents steatosis in Otsuka Long-Evans Tokushima Fatty rats. *Am J Physiol Gastrointest Liver Physiol* **294**, G619–G626.
- Rector RS, Thyfault JP, Uptergrove GM, Morris EM, Naples SP, Borengasser SJ, Mikus CR, Laye MJ, Laughlin MH, Booth FW & Ibdah JA (2010). Mitochondrial dysfunction precedes insulin resistance and hepatic steatosis and contributes to the natural history of non-alcoholic fatty liver disease in an obese rodent model. *J Hepatol* **52**, 727–736.
- Ren YY, Overmyer KA, Qi NR, Treutelaar MK, Heckenkamp L, Kalahar M, Koch LG, Britton SL, Burant CF & Li JZ (2013). Genetic analysis of a rat model of aerobic capacity and metabolic fitness. *PLoS One* **8**, e77588.
- Rogers KS, Higgins ES & Grogan WM (1980). Influence of dietary cholesterol on mitochondrial function in the rat. *J Nutr* **110**, 248–254.
- Roglans N, Sanguino E, Peris C, Alegret M, Vazquez M, Adzet T, Diaz C, Hernandez G, Laguna JC & Sanchez RM (2002). Atorvastatin treatment induced peroxisome proliferator-activated receptor  $\alpha$  expression and decreased plasma nonesterified fatty acids and liver triglyceride in fructose-fed rats. *J Pharmacol Exp Ther* **302**, 232–239.
- Satapati S, Kucejova B, Duarte JA, Fletcher JA, Reynolds L, Sunny NE, He T, Nair LA, Livingston K, Fu X, Merritt ME, Sherry AD, Malloy CR, Shelton JM, Lambert J, Parks EJ, Corbin I, Magnuson MA, Browning JD & Burgess SC (2015). Mitochondrial metabolism mediates oxidative stress and inflammation in fatty liver. *J Clin Invest* **125**, 4447–4462.
- Satapati S, Sunny NE, Kucejova B, Fu X, He TT, Mendez-Lucas A, Shelton JM, Perales JC, Browning JD & Burgess SC (2012). Elevated TCA cycle function in the pathology of diet-induced hepatic insulin resistance and fatty liver. *J Lipid Res* **53**, 1080–1092.
- Srere PA (1969). Citrate synthase. *Methods Enzymol* **13**, 3–11.
- Thyfault JP, Rector RS, Uptergrove GM, Borengasser SJ, Morris EM, Wei Y, Laye MJ, Burant CF, Qi NR, Ridenhour SE, Koch LG, Britton SL & Ibdah JA (2009). Rats selectively bred for low aerobic capacity have reduced hepatic mitochondrial oxidative capacity and susceptibility to hepatic steatosis and injury. *J Physiol* **587**, 1805–1816.
- Vieira-Potter VJ, Padilla J, Park YM, Welly RJ, Scroggins RJ, Britton SL, Koch LG, Jenkins NT, Crissey JM, Zidon T, Morris EM, Meers GM & Thyfault JP (2015). Female rats selectively bred for high intrinsic aerobic fitness are protected from ovariectomy-associated metabolic dysfunction. *Am J Physiol Regul Integr Comp Physiol* **308**, R530–R542.
- Wisloff U, Najjar SM, Ellingsen O, Haram PM, Swoap S, Al-Share Q, Fernstrom M, Rezaei K, Lee SJ, Koch LG & Britton SL (2005). Cardiovascular risk factors emerge after artificial selection for low aerobic capacity. *Science* **307**, 418–420.

## Additional information

### Competing interests

The authors have no conflicts of interest to disclose for this research.

### Author contributions

Animal feeding and initial *ex vivo* experimentation was performed at Harry S. Truman Memorial VA Hospital. Liver nucleotide and acyl-carnitine analysis was performed at University of Texas Southwestern. Additional analysis was performed at the University of Kansas Medical Center. E.M.M., R.S.R., J.P.T., conception and design of research; J.P.T., approved research design; E.M.M., C.S.C., J.A.A., M.L.G., J.A.F., X.F., performed experiments; E.M.M., C.S.C., J.A.A., M.L.G., J.A.F., X.F., analysed data; E.M.M., C.S.C., J.A.A., M.L.G., L.G.K., S.L.B., J.A.F., X.F., W.X.D., S.C.B., R.S.R., J.P.T., interpreted results of experiments; E.M.M. prepared manuscript; E.M.M., C.S.C., J.A.A., M.L.G., L.G.K., S.L.B., J.A.F., X.F., W.X.D., S.C.B., R.S.R., J.P.T. edited and revised manuscript. All authors have approved the final version of the manuscript and agree to be accountable for all aspects of the work. All persons designated

as authors qualify for authorship, and all those who qualify for authorship are listed.

### Funding

This work was partially supported by NIH DK088940 (J.P.T.), NIH 5T32AR48523-8 (E.M.M.), AHA 14POST20110034 (E.M.M.), VHA-CDA2 IK2BX001299 (R.S.R.), and VA Merit Review; 1I01BX002567-01 (J.P.T.), NIH RO1DK078184 (S.C.B.), and the Robert A. Welch Foundation I-1804 (SCB). This work was supported with resources and the use of facilities at the Harry S. Truman Memorial VA Hospital in Columbia, MO. The LCR-HCR rat model system was funded by the

Office of Research Infrastructure Programs grant P40OD021331 (L.G.K. and S.L.B.) from the National Institutes of Health.

### Acknowledgements

We acknowledge the expert care of the rat colony provided by Molly Kalahar and Lori Heckenkamp. Contact L.G.K. (lgkoch@umich.edu) or S.L.B. (brittons@umich.edu) for information on the LCR and HCR rats: these rat models are maintained as an international resource with support from the Department of Anaesthesiology at the University of Michigan, Ann Arbor, MI.